Published OnlineFirst January 22, 2019; DOI: 10.1158/1078-0432.CCR-18-2906

Translational Cancer Mechanisms and Therapy

Clinical Cancer Research

YH25448, an Irreversible EGFR-TKI with Potent Intracranial Activity in EGFR Mutant Non–Small Cell Lung Cancer

Jiyeon Yun[1], Min Hee Hong[1,2], Seok-Young Kim[1], Chae-Won Park[1], Soyoung Kim[1], Mi Ran Yun[1,3], Han Na Kang[1,3], Kyoung-Ho Pyo[1], Sung Sook Lee[4], Jong Sung Koh[5], Ho-Juhn Song[5], Dong Kyun Kim[6], Young-Sung Lee[6], Se-Woong Oh[6], Soongyu Choi[6], Hye Ryun Kim[1,2], and Byoung Chul Cho[1,2,3]

Abstract

Purpose: Given that osimertinib is the only approved third-generation EGFR-TKI against *EGFR* activating and resistant T790M mutated non–small cell lung cancer (NSCLC), additional mutant-selective inhibitors with a higher efficacy, especially for brain metastases, with favorable toxicity profile are still needed. In this study, we investigated the antitumor efficacy of YH25448, an oral, mutant-selective, irreversible third-generation EGFR-TKI in preclinical models.

Experimental Design: Antitumor activity of YH25448 was investigated *in vitro* using mutant *EGFR*-expressing Ba/F3 cells and various lung cancer cell lines. *In vivo* antitumor efficacy, ability to penetrate the blood–brain barrier (BBB), and skin toxicity of YH25448 were examined and compared with those of osimertinib using cell lines and PDX model.

Results: Compared with osimertinib, YH25448 showed a higher selectivity and potency in kinase assay and mutant *EGFR*-expressing Ba/F3 cells. In various cell line models harboring *EGFR* activating and T790M mutation, YH25448 effectively inhibited EGFR downstream signaling pathways, leading to cellular apoptosis. When compared *in vivo* at equimolar concentrations, YH25448 produced significantly better tumor regression than osimertinib. Importantly, YH25448 induced profound tumor regression in brain metastasis model with excellent brain/plasma and tumor/brain area under the concentration–time curve value. YH25448 rarely suppressed the levels of p-EGFR in hair follicles, leading to less keratosis than osimertinib in animal model. The potent systemic and intracranial activity of YH25448 has been shown in an ongoing phase I/II clinical trial for advanced *EGFR* T790M mutated NSCLC (NCT03046992).

Conclusions: Our findings suggest that YH25448 is a promising third-generation EGFR inhibitor, which may be more effective and better tolerated than the currently approved osimertinib.

Introduction

EGFR-TKI is an established first-line therapy for non–small-cell lung cancer (NSCLC) with activating *EGFR* mutations, including an exon 19 deletion (Del19) and the L858R mutation (1). Treatment of first-generation (e.g., gefitinib or erlotinib) and second-generation (e.g., afatinib or dacomitinib) EGFR-TKIs have remarkably improved survival in advanced EGFR mutant NSCLC patients (2–5).

Despite dramatic initial tumor response, the majority of patients inevitably experience disease progression after 9 to 13 months of treatment. Molecular mechanisms of acquired resistance to EGFR-TKIs involve drug target alterations (e.g., *EGFR* T790M mutation) or bypass signaling activations (e.g., *MET* amplification, *ERBB2* amplification). The gatekeeper T790M mutation in EGFR kinase is the most common (approximately 60%) resistance mechanism following first- and second-generation EGFR-TKI treatment (6, 7). Therefore, efforts have been made to target the *EGFR* T790M mutation, resulting in the development of third-generation EGFR-TKIs, including rociletinib (CO-1686), olmutinib (HM61713), and osimertinib (AZD9291; refs. 8–10). Unlike the first-/second-generation EGFR-TKIs, the third-generation EGFR-TKIs irreversibly inhibit activating *EGFR* mutations and T790M mutation, while sparing wild-type (WT) *EGFR*. Unfortunately, clinical developments of rociletinib and olmutinib have been terminated due to their disappointing efficacy and/or safety profile (11). Nevertheless, osimertinib has been successfully developed for NSCLC with T790M mutation and activating *EGFR* mutations. In AURA3 trial (second line phase III trial), osimertinib demonstrated significant progression-free survival (PFS)

[1]Yonsei Cancer Research Institute, Yonsei University College of Medicine, Seoul, Republic of Korea. [2]Division of Medical Oncology, Department of Internal Medicine, Yonsei Cancer Center, Yonsei University College of Medicine, Seoul, Korea. [3]JE-UK Institute for Cancer Research, JEUK Co. Ltd., Gumi-City, Kyungbuk, Republic of Korea. [4]Department of Hematology-Oncology Inje University Haeundae Paik Hospital, Busan, Korea. [5]Genosco Inc., Cambridge, MA. [6]Yuhan R&D Institute, Yuhan Corporation, Seoul, Korea.

Note: Supplementary data for this article are available at Clinical Cancer Research Online (http://clincancerres.aacrjournals.org/).

J. Yun and M.H. Hong contributed equally to this article and should be considered co-first authors.

H.R. Kim and B.C. Cho contributed equally to this article and should be considered co-corresponding authors.

Corresponding Authors: Byoung Chul Cho, Yonsei University College of Medicine, 51 Yonseiro, Seodaemun-gu, Seoul 120-752, Korea. Phone: 82-2-2228-8126; Fax: 82-2-393-3652; E-mail: cbc1971@yuhs.ac; and Hye Ryun Kim, nobelg@yuhs.ac

doi: 10.1158/1078-0432.CCR-18-2906

Published OnlineFirst January 22, 2019; DOI: 10.1158/1078-0432.CCR-18-2906

Translational Relevance

The *EGFR* mutations hold the largest molecular subtype of NSCLC. Despite the evolutionary development of EGFR blockade in *EGFR*-mutant NSCLC, acquired resistance is inevitably developed. Approximately 50% to 60% of patients have T790M mutation as an acquired resistant mechanism to first- and second-generation EGFR-TKIs. In this situation, osimertinib is the only FDA-approved third-generation EGFR-TKI for T790M mutant NSCLC. However, the drug still shows residual activity against wild-type *EGFR* and its efficacy is unproven in patients with leptomeningeal carcinomatosis. In our study, YH25448 demonstrated a higher efficacy, especially for brain metastasis, and better selectivity for T790M mutant *EGFR* than osimertinib did in various preclinical models of *EGFR* mutated lung cancer, highlighting its potential as best-in-class third-generation EGFR-TKI.

benefit, compared with chemotherapy, in *EGFR* T790M-mutant NSCLC (12). Furthermore, in FLAURA trial (first line phase III trial; ref. 13), osimertinib significantly improved PFS compared with first-generation EGFR-TKIs. Based on these two pivotal trials, osimertinib has become a standard of care for T790M-mutant NSCLC or a preferred option for treatment-naïve *EGFR*-mutant NSCLC (14).

Although osimertinib is the only currently approved EGFR-TKI indicated for T790M-mutant NSCLC, it is far from being perfect in terms of toxicity. In AURA3 trial (12), osimertinib treatment produced diarrhea and skin rash, albeit grade 1 or 2, in 41% and 34% of patients, respectively. The incidence of these adverse events seemed numerically higher in the FLAURA trial (13). Furthermore, QT prolongation possibly mediated by HER2 inhibitory effects of osimertinib occurred in 4% of patients in the AURA3 and FLAURA trials (12, 13). Importantly, osimertinib in combination with PD-L1 immune checkpoint inhibitor produced high incidence of interstitial pneumonitis, which may be associated with high concentration (~10% of parent) of a metabolite AZ5104 (15).

In addition to its toxicity, osimertinib also has parts to be improved for intracranial efficacy. Because brain is shielded by the blood–brain barrier (BBB), brain is considered a major pharmacologic sanctuary, likely explaining why the brain is a frequent site of failure after clinical benefit with first-/second-generation EGFR-TKIs (8). Indeed, more than 30% of patients with *EGFR*-mutant NSCLC experience disease progression during EGFR-TKI treatment due to brain metastases (BM; refs. 16, 17). Moreover, isolated BM often occurs in the presence of continued systemic control. Brain-to-plasma concentration ratio of first-/second-generation EGFR-TKIs is very low, and this suggests that frequent BM during EGFR-TKI treatment is likely due to poor BBB penetration and brain exposure with EGFR-TKIs (18, 19).

Although preclinical data demonstrated greater BBB penetration and brain exposure with osimertinib than with gefitinib, rociletinib, or afatinib (20), no prospective clinical validation has been performed. Furthermore, osimertinib has been known to be a substrate for both MDR1 (P-gp) and BCRP, which are efflux transporters of drugs at BBB (20). Therefore, given the high incidence of BM and poor prognosis in *EGFR*-mutant NSCLC (21), there is a clinical need for novel EGFR-TKIs with improved efficacy against brain lesions.

Here, we demonstrated superior antitumor activity with potent BBB penetration and better skin toxicity of YH25448, a novel mono-anilino–pyrimidine irreversible mutant-selective EGFR-TKI, compared with osimertinib, using various *in vitro* cell lines and *in vivo* mouse models. We also presented a case with T790M-mutant NSCLC who exhibited a dramatic systemic and intracranial response to YH25448 in ongoing phase I/II clinical trial (NCT03046992; ref. 26).

Materials and Methods

Cell cultures and reagents

H2291 and H1975 cells were purchased from the ATCC. The Ba/F3 cell lines were purchased from the German Collection of Microorganisms and Cell Cultures. PC9 and PC9GR cells were provided by J.C. Lee (Korea Institute of Radiological and Medical Science, Seoul, Korea). All cell lines were maintained in RPMI1640 medium supplemented with 10% FBS and 1% solution of antibiotics in a humidified incubator with 5% CO_2. All reference compounds were purchased from Selleckchem, except YH25448, which was provided by Yuhan Corporation.

Patient-derived cells

YU-1098, YU-1153, YU-1150, YU-1092, YU-1099, and YU-1097 cell lines were derived from malignant effusions of patients with NSCLC. Patient-derived cells (PDC) were initially cultured on collagen-coated plates in ACL4 medium supplemented with 5% FBS. YUX-1024 cell line was derived from its PDX model. The cells maintained the driver oncogenes that were observed in the patients. When cells were enriched in an epithelial cell adhesion molecule (EpCAM)-positive cell population with a purity of over 95%, cells were subjected to further assays. All patient samples were obtained after written informed consent from the patients using protocols approved by the institutional review board.

Kinase assay

Cell-free kinase assays were conducted using Lance Ultra time-resolved fluorescence resonance energy transfer (TR-FRET) technology from Perkin-Elmer. Briefly, each EGFR enzyme WT, single mutant (Del19, L858R, and T790M), double mutant (L858R/T790M, Del19/T790M), Her2 or Her4, serial diluted EGFR inhibitors, substrate of ULight-poly-GT peptide and variable amounts of ATP (8.5–1,088 μmol/L) were mixed in kinase assay buffer (50 mmol/L HEPES pH 7.5, 10 mmol/L $MgCl_2$, 1 mmol/L EGTA, 2 mmol/L DTT, and 0.01% Tween-20) and were added to a 96-well plate. Kinase reactions were incubated at room temperature for 1 hour and then stopped by the addition of 5 μL of 10 mmol/L EDTA. The specific Europium-labeled-anti-phosphopeptide antibody (Perkin-Elmer) diluted in LANCE detection buffer was then added to a final concentration of 2 nmol/L. After 30-minute incubation, the LANCE signal was measured on an EnVision Multilabel Reader (Perkin-Elmer). Excitation wavelength was set at 320 nm and emission monitored at 615 nm (donor) and 665 nm (acceptor). The IC_{50} values were determined using GraphPad Prism (Ver. 5, GraphPad Software Inc.).

Antiproliferation assay

Human NSCLC cell lines or PDCs with an *EGFR* mutation were incubated with test compounds. Cells were seeded onto 96-well

Published OnlineFirst January 22, 2019; DOI: 10.1158/1078-0432.CCR-18-2906

plates in 100 μL. After treatment with compounds for 72 hours, cell viability was measured by quantifying the total amount of ATP using the CellTiter-Glo 2.0 Assay Kit (Promega) per the manufacturer's instruction. Dose–response curves were fitted to the data using the GraphPad Prism (Ver. 5, GraphPad Software Inc.).

Antibodies

Primary antibodies specific for p-EGFR (Y1068; 3777), EGFR (4267), p-ERK (T202/Y204; 4370), ERK (9107), p-AKT (S473; 9271), and AKT (9272) were purchased from Cell Signaling Technologies.

H1975 subcutaneous implantation and brain metastasis (BM) model

H1975-luc human NSCLC cells were implanted into the right flank and/or brain of female BALB/c nude mice. The tumor burden of intracranial lesions and the tumor size in the right flank were measured using a BLI technique with a real time *in vivo* imaging system (IVIS Spectrum; Caliper Life Sciences) and a digital calipers (Mitutoyo Corp.), respectively. Tumor-bearing mice were treated with a once-daily oral dose of YH25448 or osimertinib from 13 days postimplantation.

In vivo pharmacodynamic study

In the H1975 human NSCLC subcutaneous xenograft model, tumor tissues treated with vehicle, YH25448, or osimertinib (3 or 10 mg/kg) were collected at 2 and 24 hours after 14 days of treatment, and EGFR downstream signals were evaluated by immunoblotting.

Pharmacokinetics

Blood, tumor, and brain samples were collected from the animals at designated time points, and the concentration of YH25448 was determined using a validated LC/MS-MS method.

Patients

The clinical study (NCT03046992) was approved by appropriate institutional review boards at each participating sites and conducted in accordance with good clinical practice guidelines and the ethical principles of the Declaration of Helsinki. All patients provided written informed consent.

Statistical analysis

All data are presented as the mean ± SEM. Data were analyzed by one-way ANOVA, followed by the Dunnett test or Student *t* test. Survival analysis was performed using a Kaplan–Meier survival curve and a log-rank test comparing each group.

Results

YH25448 is a novel irreversible inhibitor selectively targeting mutant *EGFR*s

We screened a novel series of highly potent small-molecule inhibitors, which selectively target EGFR tyrosine kinases with sensitizing and T790M mutations over WT *EGFR*. The compounds targeted the Cys797 residue in the ATP-binding site of the EGFR kinase domain and were irreversibly bound to it through a covalent bond (Fig. 1A). In particular, the aminopyrimidine moiety of YH25448 bound to the hinge residue Met793 through hydrogen bonding. The phenyl substituent in the pyrazole ring pointed to the gatekeeper residue Met790. The morpholine ring faced the solvent exposure region, and the *meta*-acrylamide formed a covalent bond with Cys797.

To investigate YH25448 *in vitro* profiles for various targets, we performed kinome profiling of a single-dose inhibition assay against 304 kinases, including WT and mutant EGFRs. The levels of inhibition of kinase activities by 1 μmol/L YH25448, tested in duplicate, were compared with those of the DMSO control (0% inhibition). The average values were plotted, with a 65% cutoff value, in a representation of the human kinome phylogenetic tree using TREEspot from DiscoveRx (Fig. 1B). Although osimertinib displayed a broad inhibition profile against 17 kinases, YH25448 had a relatively higher kinase selectivity profile, than osimertinib, based on the finding that it inhibited 11 of the 304 kinases tested (Fig. 1C). In particular, YH25448 at a concentration of 1 μmol/L potently inhibited kinase activities of *EGFR* T790M, L858R/T790M, and L858R, and mitogen-activated protein kinase kinase kinase MAP3K9 (MLK1), with the respective percentages of inhibition exceeding 90% and an S-score of 0.03. *EGFR* T790M was the only protein kinase inhibited at a very high level (above 98%). *EGFR* L858R/T790M and L858R were also found among the hits, with 98% and 91% inhibition, respectively. Although YH25448 showed a high selectivity and a strong activity against the various mutant *EGFR*s, it exhibited less activity against WT *EGFR*, compared with that of osimertinib (Fig. 1C). This finding suggested that YH25448 might decrease off-target side effects compared with that of osimertinib. To validate the results of kinome profiling, we carried out cell-free *in vitro* kinase inhibition assays for mutant *EGFR*s and the ErbB family with serially diluted YH25448 and osimertinib (Table 1A). Compared with those of osimertinib, YH25448 showed similar or greater potencies in the inhibition of kinase activities of mutant *EGFR*s, including Del19, L858R, and T790M mutants, with the half-maximal inhibitory concentration (IC_{50}) values ranging from 1.7 to 20.6 nmol/L. Individual EGFR kinase inhibition assay for rare mutant *EGFR*s that are shown in NSCLC demonstrated that the active metabolite of YH25448 (YH26334) effectively inhibited the rare *EGFR* mutants at low concentration. On the contrary, we found that the activity of YH25448 (YH26334) for WT EGFR was lower compared with those of osimertinib (AZ5104), indicating that higher selectivity of the active metabolite of YH25448 for mutant *EGFR* might reduce the possibility of adverse effect of the drug (Table 1B).

Consistent with the data from the cell-free *in vitro* kinase assay, YH25448 significantly and dose dependently inhibited the EGFR phosphorylation in Ba/F3 cells harboring the Del19, L858R, Del19/T790M, and L858R/T790M mutations (Fig. 1D). The viability of the Ba/F3 cells with the mutant *EGFR*s was remarkably reduced by YH25448, with the mean IC_{50} values ranging from 3.3 to 5.71 nmol/L (Fig. 1E), which were similar to those obtained for osimertinib-treated cells (Table 2). As previously reported (22, 23), the first-generation TKI gefitinib was overall ineffective at inhibiting the growth of Ba/F3 cells with T790M mutant *EGFR*s.

Collectively, these findings suggest that YH25448 is a novel mutant-selective EGFR inhibitor with selectivity and potency at least comparable to osimertinib, which is a currently approved third-generation EGFR-TKI.

YH25448 significantly suppresses *EGFR*-mutant lung cancer in *in vitro* and *in vivo*

To investigate whether YH25448 could effectively block EGFR and its downstream signaling pathways, we treated *EGFR*-mutant

Published OnlineFirst January 22, 2019; DOI: 10.1158/1078-0432.CCR-18-2906

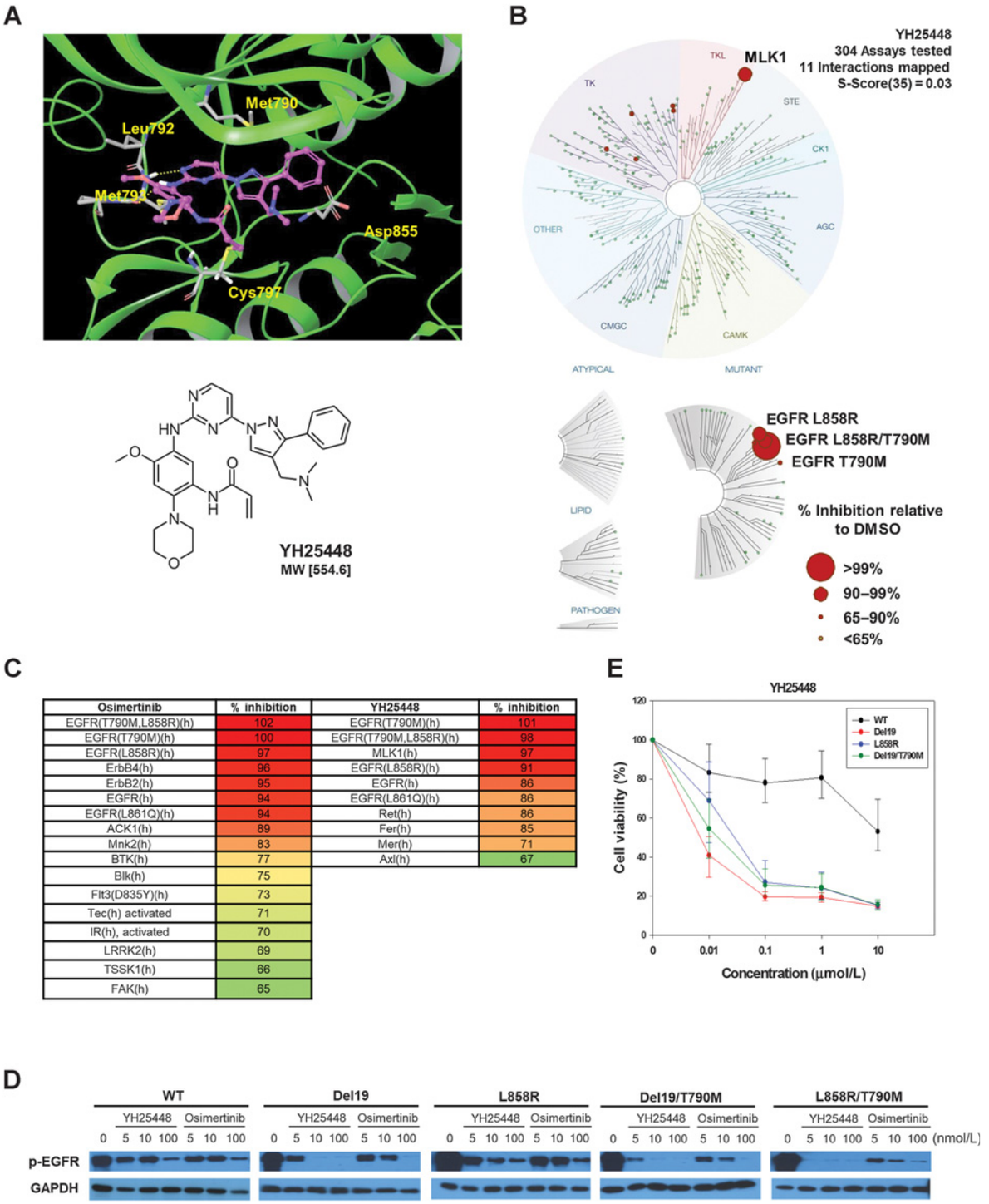

Osimertinib	% inhibition	YH25448	% inhibition
EGFR(T790M,L858R)(h)	102	EGFR(T790M)(h)	101
EGFR(T790M)(h)	100	EGFR(T790M,L858R)(h)	98
EGFR(L858R)(h)	97	MLK1(h)	97
ErbB4(h)	96	EGFR(L858R)(h)	91
ErbB2(h)	95	EGFR(h)	86
EGFR(h)	94	EGFR(L861Q)(h)	86
EGFR(L861Q)(h)	94	Ret(h)	86
ACK1(h)	89	Fer(h)	85
Mnk2(h)	83	Mer(h)	71
BTK(h)	77	Axl(h)	67
Blk(h)	75		
Flt3(D835Y)(h)	73		
Tec(h) activated	71		
IR(h), activated	70		
LRRK2(h)	69		
TSSK1(h)	66		
FAK(h)	65		

Figure 1.

Characterization of the EGFR mutant-selective irreversible inhibitor YH25448. **A,** Crystal structure of YH25448 in a complex with the EGFR T790M mutant (top). Chemical structure of YH25448 (bottom). **B,** Kinome tree for YH25448 generated using DiscoveRx TREEspot version 4. Sizes of the red circles are proportional to the percentage inhibition at the test concentration (1 μmol/L): largest circle, 99% inhibition; medium circle, 90% to 99% inhibition; smallest circles, 65% to 90% inhibition. **C,** Comparison of YH25448 and osimertinib selectivity profiles against approximately 320 kinases. The kinases listed were subject to over 65% inhibition by each compound, compared with DMSO. **D,** Ba/F3 cells overexpressing the indicated *EGFR* mutant were treated with YH25448 or osimertinib for 6 hours at the indicated concentrations. p-EGFR levels were detected by Western blot analysis. **E,** Viability of Ba/F3 cells was determined via Cell Titer Glo. YH25448 was treated for 72 hours.

Published OnlineFirst January 22, 2019; DOI: 10.1158/1078-0432.CCR-18-2906

Table 1. YH25448 selectively inhibits EGFR mutant

A

	IC_{50}, nmol/L	
EGFR kinase genotype	**YH25448**	**Osimertinib**
Wild type	76.0	54.0
Del19	5.3	8.6
L858R	20.6	12.2
Del19/T790M	1.7	2.2
L858R/T790M	2.0	8.0
ErbB2	364.0	44.0
ErbB4	1,017.0	54.0

B

EGFR kinase genotype	**YH25448**	**YH26334[a]**	**Osimertinib**	**AZ5104[b]**
EGFR (wild type)	60	91	20	0.98
EGFR (G719C)	1.7	4.8	65	4.2
EGFR (G719S)	4.1	9.3	49	3.2
EGFR (E746-A750del)	0.43	1.8	3.7	0.69
EGFR (L747-E749del, A750P)	14	38	3.2	0.53
EGFR (L747-S752del, P753S)	14	16	4.4	0.39
EGFR (L747-T751del, Sins)	8.3	13	4.9	1.1
EGFR (S752-I759del)	96	91	6.4	1.1
EGFR (L861Q)	14	22	5.6	0.54

IC_{50} values of YH25448 and osimertinib.

Each value represents the mean ± SEM calculated from at least two independent experiments.

[a]The active metabolite of YH25448 (YH26334) is present in humans at levels approximately 3% those of the parent (NCT03046992).

[b]The active metabolite of osimertinib (AZ5104) is present in humans at levels approximately 10% those of the parent.

lung cancer cells with YH25448 at different concentrations for 6 hours (Fig. 2A). YH25448 significantly suppressed EGFR downstream signaling, including phospho-EGFR (p-EGFR), phospho-AKT (p-AKT), and phospho-ERK (p-ERK). The inhibitory effects of YH25448 were stronger than or comparable to those of osimertinib under the same conditions. In contrast, YH25448 did not inhibit EGFR signaling in a WT EGFR cell line (H2291). We further explored whether the blockade of EGFR signaling by YH25448 in lung cancer cell lines correlated with its inhibitory effects on cell proliferation in various NSCLC cell lines including six PDCs harboring with sensitizing *EGFR* mutations [Del19 (YU-1098), L858R (YUX-1024)], resistant mutations [Del19/T790M (YU-1153), L858R/T790M (YU-1150), Del19/T790M/C797S (YU-1097)], and uncommon mutations [L861Q (YU-1092), G719C/S768I (YU-1099); Fig. 2B; Sanger sequencing results shown in Supplementary Fig. S1A]. The cell viability data showed that YH25448 effectively and significantly inhibited the proliferation of Del19- and/or T790M-mutant NSCLC cells at lower concentrations than those needed to inhibit cells with other EGFR-TKIs (IC_{50} values ranging from 1.9 to 12.4 nmol/L against PC9, YU-1098, PC9GR, YU-1153, and YU-1150), while showing much less activity against cells with WT *EGFR* (H2291; Fig. 2B). YH25448 exhibited modest antiproliferative effects in PDCs (YU-1092 and YU-1099) harboring uncommon *EGFR* mutations with IC_{50} values of 42.5 and 1224.7 nmol/L, respectively. As previously reported (24), L861Q-mutant lung cancer cells (YU-1092) showed significant inhibition to afatinib. YU-1097 derived from an patient with osimertinib-resistant NSCLC showed resistance to YH25448 and other third-generation EGFR-TKIs. Treatment with YH25448 induced the apoptosis in *EGFR*-mutant cell lines, as demonstrated by an increase in the cleaved Bim-EL protein or activated caspase-3/7, in H1975 and PC9 cells (Supplementary Fig. S1B and S1C). To determine whether YH25448 is effective *in vivo*, H1975 tumor-bearing mice were randomly grouped and dosed orally, once daily, with the vehicle and 1, 3, and 10 mg/kg YH25448 or osimertinib for a period of 13 days. YH25448 significantly shrunk the tumor volume within a very short period after the first administration at doses as low as 3 and 10 mg/kg/day (Fig. 2C). After 13-day treatment at a dose of 3 mg/kg treatment, YH25448 suppressed 86.85% of the tumor growth compared with only 7.24% tumor regression in the osimertinib group. Surprisingly, near complete tumor regression (90%) was achieved at a higher dose, 10 mg/kg, without any body weight changes (Supplementary Fig. S1D). A similar degree of tumor shrinkage was observed after administration of 3 mg/kg YH25448 to a PC9 tumor-bearing xenografts after 25 days (Supplementary Fig. S1E and S1F). As shown in Fig. 2D and E, the complete inhibition of p-EGFR was observed as early as 2 hours post-dose in tumor samples from the xenografts, which were treated with YH25448 (3 or 10 mg/kg) for 3 days. The complete inhibition of p-EGFR activity was maintained until 24 hours post-dose. Although YH25448 treatment at 3 mg/kg resulted in partial inhibitions of

Table 2. Viability of Ba/F3 cells expressing WT and mutant *EGFR*s was measured via Cell Titer Glo

	IC_{50}, nmol/L		
Ba/F3_EGFR	**YH25448**	**Osimertinib**	**Gefitinib**
Wild type	722.7	519.1	585.3
Del19	3.3	3.5	10.2
L858R	3.9	3.6	71.1
Del19/T790M	4.9	3.4	769.9
L858R/T790M	5.7	4.3	7628.2

IC_{50} values (nmol/L) of YH25448, osimertinib, and gefitinib were calculated.

Published OnlineFirst January 22, 2019; DOI: 10.1158/1078-0432.CCR-18-2906

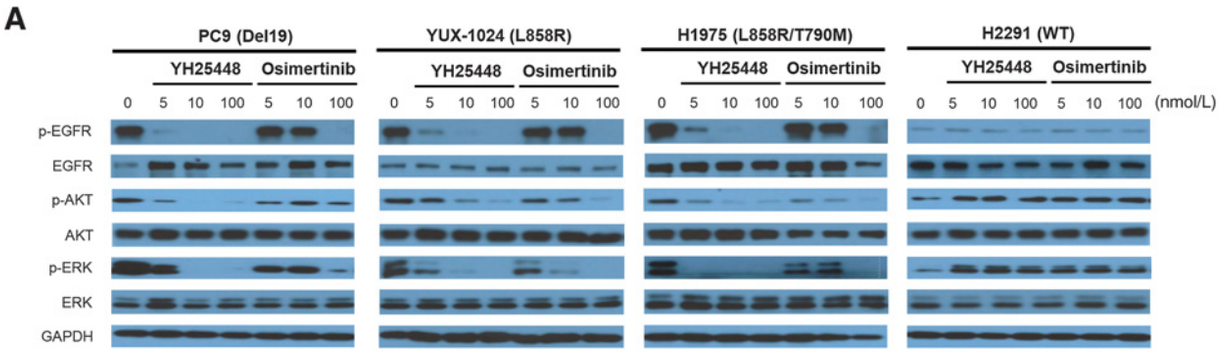

B

	Cell lines	IC_{50}, nmol/L					
		YH25448	Osimertinib	Olmutinib	Rociletinib	Afatinib	Gefitinib
	H2291 (WT)	N/A	3665.0	11854.8	4425.3	1654.5	N/A
Sensitizing	PC9 (Del19)	3.8	11.2	59.2	172.7	5.4	63.0
Sensitizing	YU-1098 (Del19)	2.8	4.4	8.4	17.5	3.3	5.5
Sensitizing	YUX-1024 (L858R)	83.7	71.0	884.1	864.3	6.9	18.0
T790M+	PC9GR (Del19/T790M)	12.4	21.1	164.7	922.8	808.0	10184.0
T790M+	YU-1153 (Del19/T790M)	4.6	3.3	4.3	10.1	329.3	6419.1
T790M+	YU-1150 (L858R/T790M)	1.9	1.6	38.7	14.3	38.0	11820.0
Uncommon	YU-1092 (L861Q)	42.5	49.8	603.2	611.5	5.9	522.5
Uncommon	YU-1099 (G719C/S768I)	1224.7	1427.8	1853.0	966.7	426.0	1914.0
C797S+	YU-1097 (Del19/T790M/C797S)	1586.7	1356.8	9399.6	1827.0	1007.5	6209.7

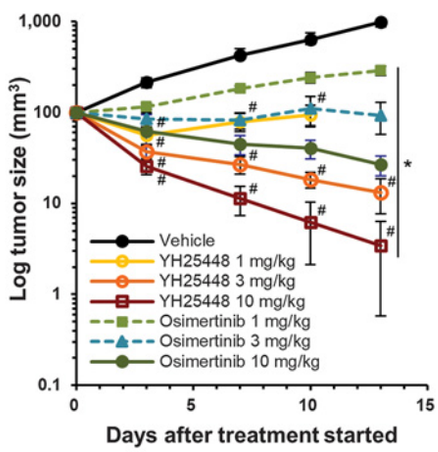

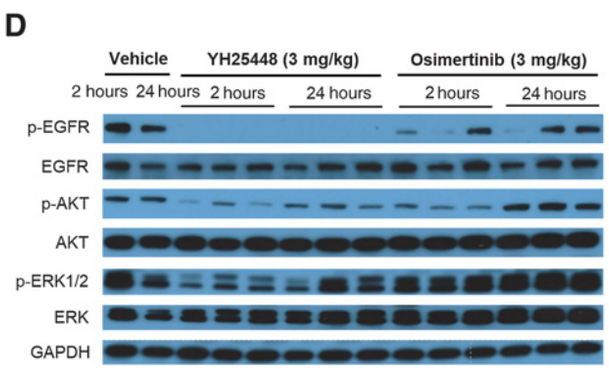

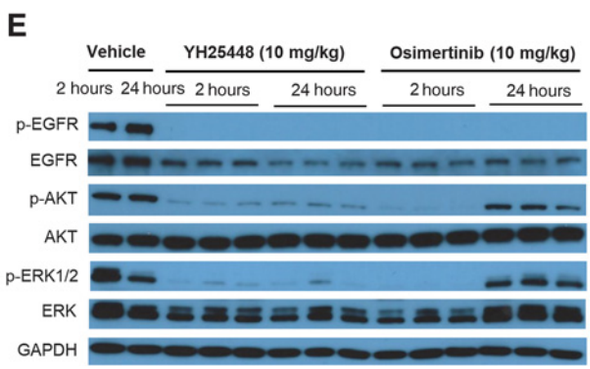

Figure 2.

Potency and selectivity of YH25448. **A,** Immunoblot analysis was performed for EGFR, AKT, and ERK expression after YH25448 or osimertinib treatment for 6 hours at the indicated concentrations in lung cancer cell lines. Antitumor effects of YH25448 in *EGFR* T790M mutant NSCLC (H1975, L858R/T790M)-bearing mice ($n = 7$/group). **B,** IC_{50} values for the indicated EGFR-TKIs in the cells (Treatment of the drugs for 72 h). **C,** Antitumor effects of YH25448 in H1975 (L858R/T790M) tumor-bearing mice ($n = 7$/group). Mice were treated with YH25448, osimertinib, or vehicle once daily for 2 weeks after the tumor volume reached 100 mm^3. Data represent the mean ± SEM ($n = 7$/group). *, $P < 0.001$ vs. vehicle control; #, $P < 0.0001$ vs. osimertinib at the same dose. **D** and **E,** Tumor lysates of vehicle-, YH25448-, or osimertinib-treated H1975 xenograft mice for 3 days were harvested at the indicated time point after the last treatment. Lysates were subjected to immunoblotting for p-EGFR (Y1068), p-AKT, and p-ERK1/2.

Published OnlineFirst January 22, 2019; DOI: 10.1158/1078-0432.CCR-18-2906

p-AKT and p-ERK1/2, samples from the mice treated with 10 mg/kg YH25448 showed complete inhibition of both signaling pathways. Comparing the inhibitory efficacy of YH25448 with that of osimertinib at the same doses and at the same time points, YH25448 effectively and comparably suppressed the signaling pathways and maintained the suppression to osimertinib did. Importantly, osimertinib-treated tumor samples showed reactivation of p-AKT and p-ERK1/2 within 24 hours, which may mediate innate/acquired resistance to osimertinib (25).

Collectively, these data indicated that YH25448 selectively and potently affected EGFR signaling and viabilities of NSCLC cells harboring sensitizing and T790M *EGFR* mutations. Our *in vitro* and *in vivo* data strongly suggests a more potent antitumor efficacy of YH25448 than osimertinib.

YH25448 shows superior tumor-regressing efficacy in an *EGFR* mutant BM model, with a high BBB penetration profile

To examine whether YH25448 has the ability to penetrate BBB *in vivo*, a BM mouse model was established by intracranial implantation of luciferase-transfected H1975 cells (H1975-luc). When bioluminescent imaging (BLI) signals reached $>3 \times 10^7$ photons/second, the mice were assigned to five different treatment groups, including the vehicle, YH25448 (10 or 25 mg/kg), and osimertinib (10 or 25 mg/kg). According to previous data, a dose of 25 mg/kg osimertinib once daily in nude mice provides the exposure level comparable to that provided by an 80-mg once-daily dose in humans (20). YH25448 more effectively inhibited intracranial tumor growth than osimertinib at 10 and 25 mg/kg once daily during a 49-day treatment ($P = 0.0125$ and 0.0274, respectively, by one-way ANOVA), with no obvious loss of the body weight (Fig. 3A and B; Supplementary Fig. S2A and S2B). Consistent with brain tumor reduction detected by BLI in the YH25448-treated mice, histologic analysis showed that the area of the brain tumor was reduced, and the number of proliferating cells also significantly decreased in the YH25448 (10 mg/kg)-treated mice compared with that in the vehicle-treated mice (Fig. 3C). To evaluate whether there is a correlation between the brain tumor regression by YH25448 treatment and the survival of the mice, we calculated the survival rates in the vehicle-treated, YH25448-treated (10 or 25 mg/kg), and osimertinib-treated (10 or 25 mg/kg) groups. Although all mice were dead in the vehicle group at 42 days after tumor implantation, the YH25448-treated mice showed significantly longer survival than osimertinib-treated mice (the median survival of the mice, 124 days vs. 65 days for osimertinib at 10 mg/kg, $P = 0.0018$; 174 days vs. 121 days for osimertinib at 25 mg/kg, $P = 0.0021$ by the *t* test; Fig. 3D). In the H1975-luc BM xenograft model, YH25448 demonstrated excellent BBB penetration. The maximum concentration of the compound was detected in the plasma, brain, and intracranial tumor after 4 hours post-dose with a single dose of 10 mg/kg. The uptake in the intracranial tumor was notably higher than that in the plasma and brain tissue. AUC_{last} ratios were calculated from *in vivo* PK bioanalytical data and presented in Fig. 3E (top), and the time–concentration profiles of the total YH25448 in the plasma, brain, and intracranial tumor are presented in Fig. 3E (bottom). The unbound brain-to-plasma ratio (Kpuu,brain) of YH25448 was 0.29 when considering the unbound fraction in plasma and brain tissue. The value was generally comparable to that of osimertinib, which result was previously reported as 0.39. The intracranial tumor/plasma and intracranial tumor/brain AUC_{last} ratios for YH25448 were 7.0 and 7.9, respectively. To verify whether YH25448 was a substrate of efflux transporters such as BCRP and MDR1 (P-gp), which are known to block any molecules to penetrate the BBB, we measured net efflux ratio (ER) of MDR1 or BCRP at different doses of YH25448 (Supplementary Fig. S2C). Based on positive substrate criteria of efflux ratio (ER > 2) and a previous report (20), whereas osimertinib was a substrate of both BCRP and MDR1 (P-gp), YH25448 was not a substrate of BCRP and only a weak substrate of MDR1. These results suggested that YH25448 may be less affected by efflux transporters.

These results suggested that YH25448 might be more effective than osimertinib in treating metastatic brain tumors from lung cancer.

YH25448 demonstrates potent antitumor activity in an *EGFR*-mutant patient-derived xenograft model and in an *EGFR* T790M-mutant NSCLC patient

To further validate antitumor activity of YH25448 *in vivo*, PDX models established from an *EGFR* Del19 mutant NSCLC patient were dosed orally with YH25448 and osimertinib at 25 mg/kg once daily for 20 days. YH25448 exhibited more potent tumor regression than osimertinib (87.5% and 83.6% inhibition of tumor growth, respectively; $P < 0.001$; Fig. 4A). Both treatments were well tolerated without a significant body weight loss (Fig. 4B).

In an ongoing phase I/II study of YH25448 in *EGFR* mutant NSCLC progressing on prior EGFR-TKI, dramatic and durable responses have been observed even at the lowest dose (20 mg, once daily; ref. 26). The first patient was a 62-year-old Korean male with *EGFR* L858R/T790M mutant lung adenocarcinoma who had progressed following 10-month treatment of gefitinib. The patient was treated with YH25448 20 mg orally once daily, resulting in 51% tumor reduction following 6-week treatment (Fig. 4C). During the treatment, the patient reported no significant adverse events and response lasted for over 8 months. The second patient was a 37-year-old Korean male with *EGFR* Del19/T790M mutant lung adenocarcinoma who had experienced systemic progression including brain following 8-month treatment of AZD3759 and 2-month treatment of gefitinib. Upon YH25448 40 mg treatment, tumor assessment confirmed a 49.3% intracranial tumor reduction, with a 12.7% extracranial tumor reduction (overall 25.9% tumor reduction) without significant adverse events (Fig. 4D).

YH25448 shows less selectivity for WT *EGFR* and less skin toxicity than osimertinib does

EGFR is widely expressed in undifferentiated, proliferating keratinocytes in the epidermis and in the outer layer of hair follicles (27). Therefore, cutaneous toxicities such as acneiform rash, itching, and xerosis are most commonly associated with EGFR-TKI treatments including osimertinib (28–31).

Following the observation that both YH25448 and osimertinib did not exhibit severe skin toxicity at 10 mg/kg YH25448 (clinical equivalent to 240 mg once daily) and 25 mg/kg osimertinib (clinical equivalent to 80 mg once daily), we escalated the dose up to 50 and 75 mg/kg to demonstrate a wider therapeutic index of YH25448 over osimertinib.

We observed that the YH25448-treated (50 mg/kg) H1975-bearing BALB/c nude mice appeared phenotypically normal. On the contrary, one of the five mice treated with osimertinib (50 mg/kg) showed minimal signs of keratosis on the skin (Fig. 5A). We further extended the experiment with the treatment of mice with a

Published OnlineFirst January 22, 2019; DOI: 10.1158/1078-0432.CCR-18-2906

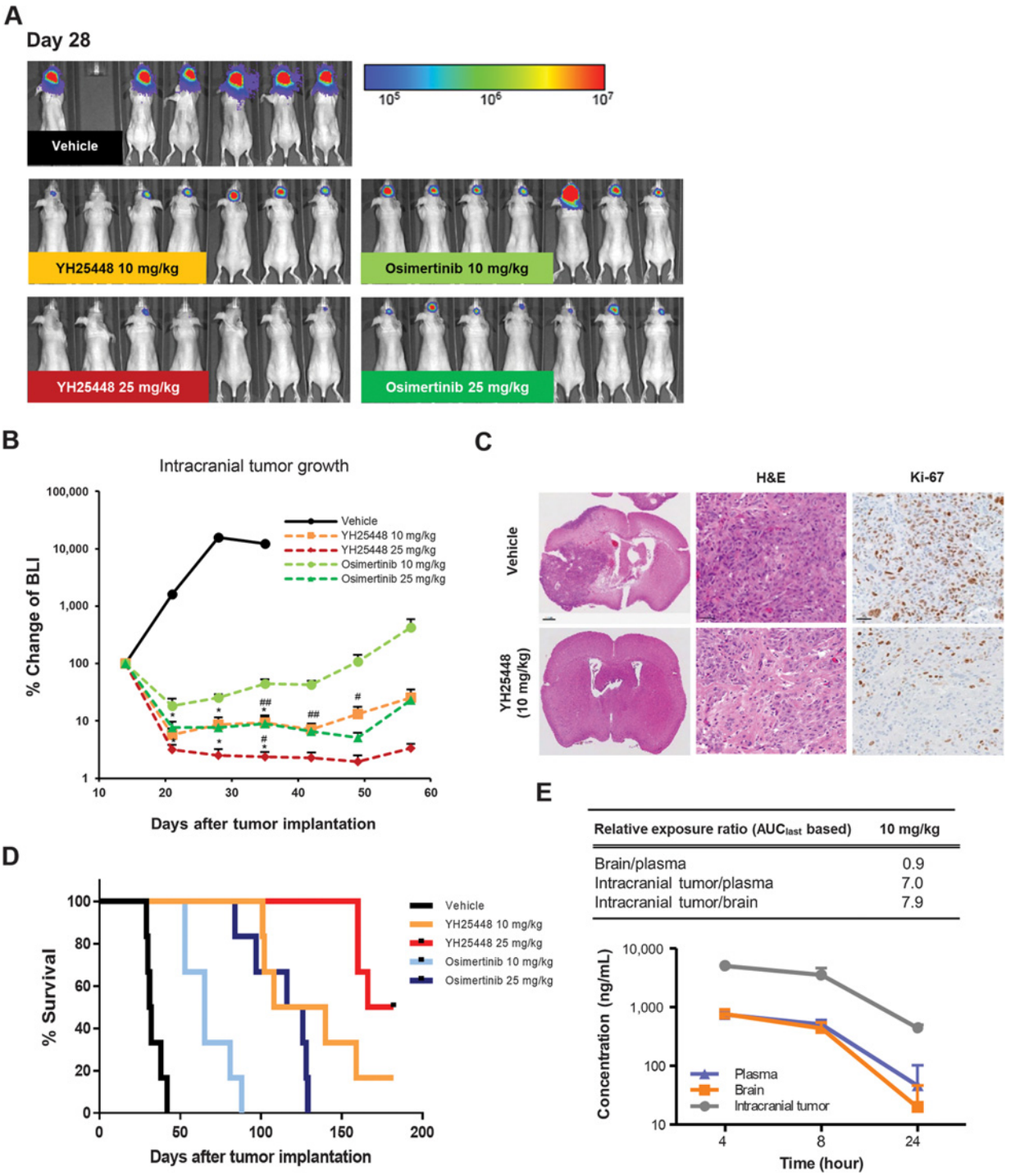

Figure 3.

Intracranial antitumor effects of YH25448 in the H1975-luc BM model. **A** and **B,** An intracranial tumor growth model was established with BALB/c nude mice using H1975-luc cells. Two weeks after H1975-luc injection, animals were treated with YH25448 or osimertinib once daily. BLI was used to detect intracranial tumor growth *in vivo*. Data represent the mean ± SEM ($n = 7$/group). *, $P < 0.001$ vs. vehicle control; #, $P < 0.01$; ##, $P < 0.05$ vs. osimertinib at the same dose. **C,** Histopathologic examination of brain sections obtained following H1975-luc intracranial implantation. H&E staining and immune histochemical staining for Ki-67. Scale bars, 25 μm. **D,** Kaplan–Meier survival curves of H1975-luc cells in mice treated with YH25448 or osimertinib at 10 and 25 mg/kg, once daily, respectively. **E,** Plasma, intracranial tumor, and brain tissue samples obtained at 4, 8, and 24 hours post dosing of YH25448 (10 mg/kg) on day 21 post-dose were analyzed with a validated LC/MS-MS method.

Published OnlineFirst January 22, 2019; DOI: 10.1158/1078-0432.CCR-18-2906

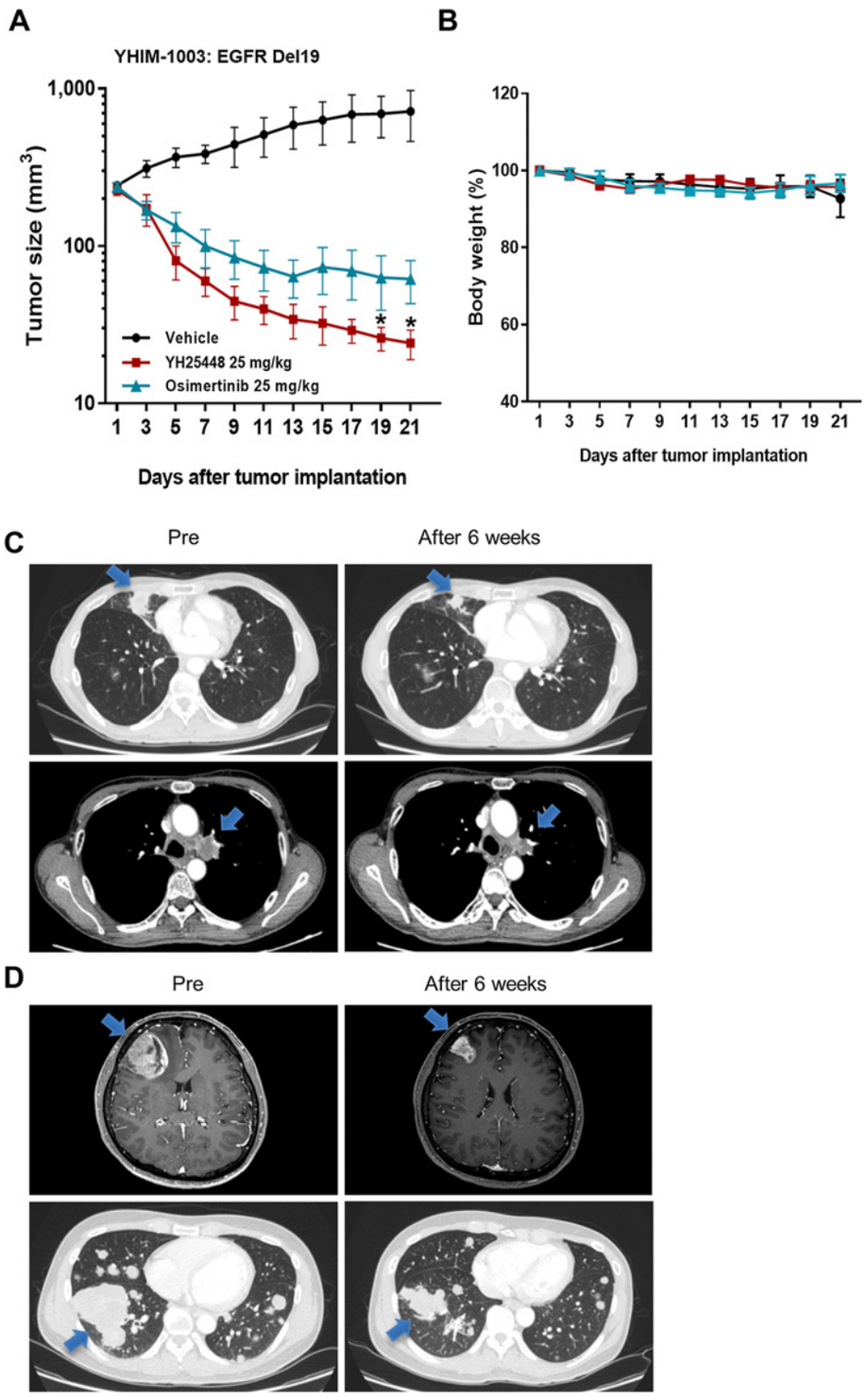

Figure 4.
Efficacy of YH25448 in a patient-derived xenograft mouse model and representative response in the patients. **A,** Patient-derived tumors implanted in mice (YHIM-1003; EGFR Del 19; passage 3) were treated with YH25448 or osimertinib at 25 mg/kg, once daily, when tumors reached 200 mm^3 in volume. Data represent the mean ± SEM ($n = 7$/group). *, $P < 0.01$ vs. osimertinib. **B,** Body weight. **C,** Radiologic response following YH25448 20 mg treatment in a 62-year-old male patient with the *EGFR* T790M mutation. **D,** Intracranial and extracranial response after YH25448 40-mg treatment in a 37-year-old male patient with the *EGFR* T790M mutation. Blue arrow indicates the tumor lesion.

75 mg/kg dose of each drug. Forty percent of the mice (2/5) in the YH25448 treatment group showed minimal keratosis, whereas severe keratosis on the face, neck, and abdomen was observed in all osimertinib-treated mice (Fig. 5A–C; Supplementary Fig. S3A). To determine whether these phenotypical differences were due to less selectivity of YH25448 for WT *EGFR*, we performed histologic examination of the skin from the mice in both groups. As shown in Fig. 5D and Supplementary Fig. S3B, at 75 mg/kg dose, YH25448 rarely suppressed the levels of p-EGFR (WT) in hair follicles, whereas osimertinib strongly reduced the

Published OnlineFirst January 22, 2019; DOI: 10.1158/1078-0432.CCR-18-2906

A

Groups	Clinical signs	Severity	Observed regions
Vehicle	-	-	-
YH25448 (50 mg/kg)	-	-	-
YH25448 (75 mg/kg)	Keratosis (2/5)	Minimal (2/5)	Abdomen (2/5)
Osimertinib (50 mg/kg)	Keratosis (1/5)	Minimal (1/5)	Left fore-arm (1/5)
Osimertinib (75 mg/kg)	Keratosis (5/5)	Severe (5/5)	Face, neck, abdomen (5/5)

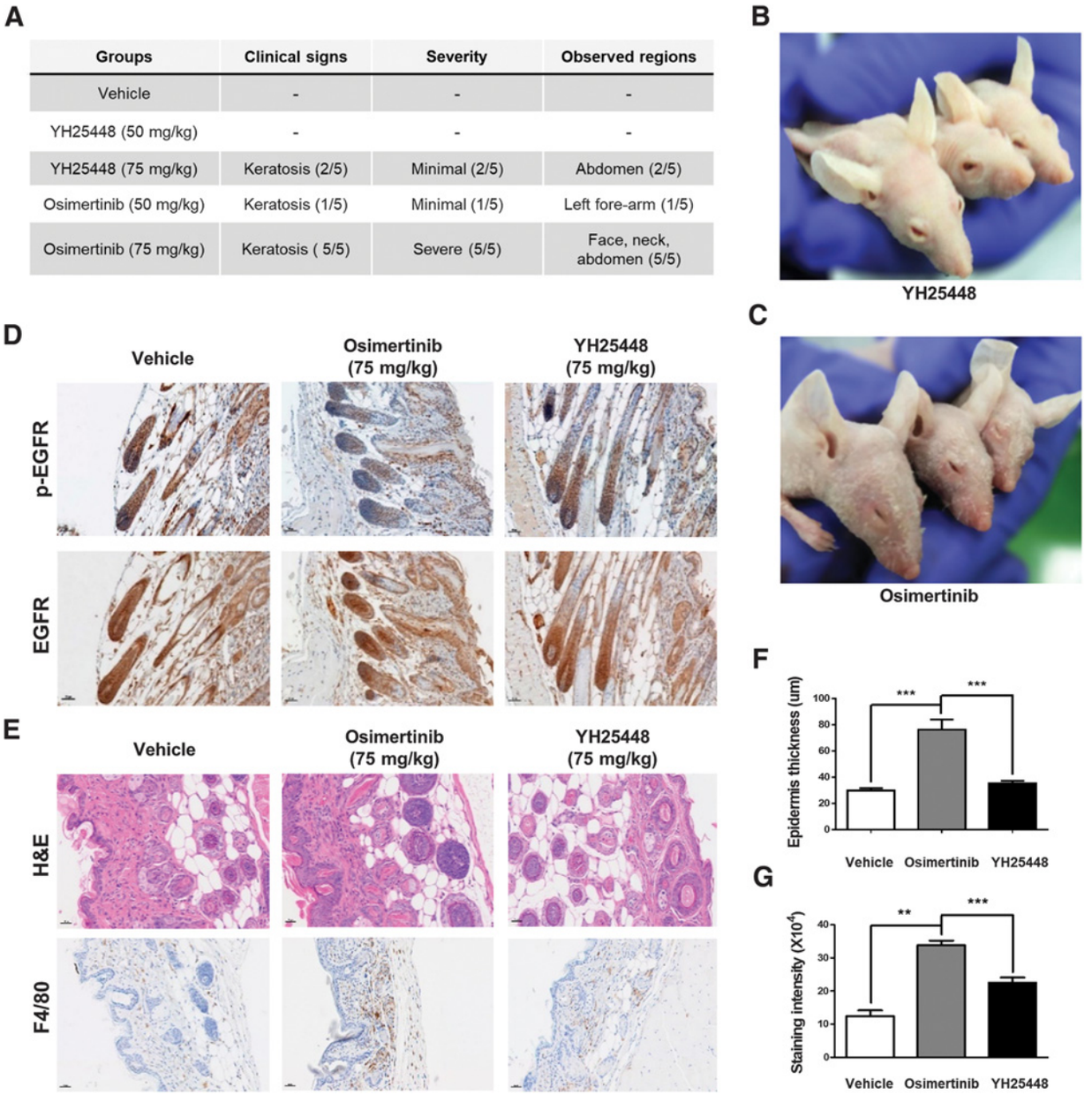

Figure 5.

YH25448 less suppresses WT EGFR than osimertinib *in vivo*. **A,** Skin problems of BALB/c nude mice-treated with vehicle, YH25448 (50 and 75 mg/kg), or osimertinib (50 and 75 mg/kg). **B** and **C,** Representative photographs of 75 mg/kg YH25448 or osimertinib-treated BALB/c nude mice after 12 days. Photos taken from separate experiment to **D–G**, but study design was very similar. **D** and **E,** Immunohistochemical analysis of mouse skin for p-EGFR, EGFR, F4/80 and H&E staining results. Representative images are presented. **F** and **G,** Histogram of staining intensity for implying the infiltrated cells in epidermis and hair follicles and epidermal thickness based on H&E staining images. Measurements were taken from five images for each group, and results are presented as mean ± SD. ***, $P < 0.0001$; **, $P < 0.00001$.

phosphorylation of EGFR (WT). Based on the results of hematoxylin and eosin (H&E) staining, the epidermis of the osimertinib-treated mice was significantly thicker than that of the YH25448-treated mice (Fig. 5E, top and 5F). From the results showing that a higher H&E staining intensity observed in the epidermis of osimertinib-treated mice than that of YH25448-treated mice (Fig. 5G), we predicted strong infiltration of immune cells by osimertinib, compared with YH25448 did. The blockade of EGFR leads to the upregulation of chemokine expression and massive infiltration of T cells and macrophages into the skin, which causes skin inflammation (32). Because BALB/c nude mice were used for these experiments, we were only able to test the levels of macrophages (detected with F4/80 antibody) infiltrated into the dermis in each group. Consistent with the above data,

Published OnlineFirst January 22, 2019; DOI: 10.1158/1078-0432.CCR-18-2906

YH25448 did not affect the macrophage infiltration in the epidermis (Fig. 5E; bottom). However, osimertinib enhanced the macrophage infiltration at the same dose, indicating that the inflammation caused by macrophage occurred in the osimertinib-treated mice, which thickened the epidermis.

Taken together, these data strongly suggest that YH25448 has less selectivity for WT *EGFR*, resulting in less cutaneous toxicity than osimertinib at high doses.

Discussion

In this study, we comprehensively analyzed the selective antitumor activity of YH25448 against *EGFR* sensitizing- and T790M-mutant NSCLC using kinase assays, various patient-derived cell line/xenografts, and patient cases enrolled in an ongoing phase I/II study. Our findings suggest that YH25448 had a superior preclinical activity and safety to osimertinib, which is a current standard of care for T790M-mutant NSCLC (33, 34).

Given the frequent CNS progression while EGFR-TKI treatment (16, 17), AUC-based brain-to-plasma ratio (0.9) and intracranial tumor-to-plasma ratio (7.0) of YH25448 shown in our study is noteworthy (Fig. 3E). These outstanding *in vivo* PK parameters were supported by superior CNS activity of YH25448 in H1975-luc BM mouse models (Fig. 3A and B) and a dramatic CNS response in a clinical case report (Fig. 4D). Furthermore, we demonstrated that YH25448 was not a substrate of BCRP and only a weak substrate of MDR1, suggesting that it may be less affected by efflux transporters than osimertinib. Additionally, given that YH25448 at 10 mg/kg in murine approximates to the recommend clinical exposure of 240 mg once daily in clinical trial phase II, our data showed the similar antitumor efficacy in BM models (Fig. 3A, B and D) compared with 25 mg/kg osimertinib (the clinically relevant dose is 80 mg once daily). Taken together, these results suggested that at least equivalent activity of YH25448 for CNS metastasis may be expected to that of osimertinib.

In addition, YH25448 has potential advantage over osimertinib or other third-generation EGFR-TKIs in terms of toxicity. Because of the important role of EGFR signaling in skin, cutaneous toxicities have been frequently reported with the first- or second-generation EGFR-TKIs. The most frequent cutaneous toxicities are papulopustular rash, itching, and inflammation around the nails, affecting 49% to 89%, 10% to 20%, and 14% to 61%, respectively (2, 3, 5, 35, 36). Although these cutaneous toxicities seemed lower with osimertinib, it also produced papulopustular rash in 34% to 58%, itching in 13% to 18%, and inflammation around the nails in 22% to 36%, respectively (12, 13). Although rarely life-threatening, these cutaneous toxicities cause significant physical and psycho-social discomfort, which may lead to a decreased quality of life and modification or discontinuation of treatment (37). In our study, we observed that YH25448 produced less keratosis on the skin than osimertinib in H1975-bearing BALB/c nude mice (Fig. 5A–C; Supplementary Fig. S3A). By histologic examination, we demonstrated that the minimal skin toxicity in YH25448-treated mice was due to less selectivity of YH25448 for WT *EGFR* (Fig. 5D; Supplementary Fig. S3B). Indeed, unlike osimertinib, YH25448 rarely suppressed the levels of WT p-EGFR in hair follicles, leading to less macrophage-mediated cutaneous inflammation in the dermis (Fig. 5E, bottom and 5G). Although the dose of YH25448 and osimertinib used in the skin toxicity experiments was higher than the clinical equivalent doses (10 mg/kg YH25448 and 25 mg/kg osimertinib, respectively), these data supports a wider therapeutic index of YH25448, compared with osimertinib, in terms of skin toxicity. Based on our results, we expected less cutaneous toxicities in patients treated with YH25448 than those with osimertinib, which lead to improved patient's quality of life.

In addition to cutaneous toxicity, YH25448 may be associated with less cardiac dysfunction and hyperglycemia due to lack of activity on HER2 and type 1 insulin-like growth factor receptor (IGF-1R; Fig. 1C). In contrast, changes in QT interval was reported with osimertinib in 10% due to HER-2 inhibition and/or hERG channel inhibition, whereas hyperglycemia was reported with rociletinib in 47% due to IGF-1R inhibition (10, 13). Importantly, our preclinical findings were translated into promising efficacy in the phase I/II study in advanced EGFR mutant NSCLC with acquired resistance to EGFR-TKIs (26). This clinical trial included dose escalation and dose-expansion cohorts. In the expansion cohorts, tumor biopsies prior to treatment were required for central confirmation of EGFR T790M status. Among 38 patients enrolled in the dose-escalation cohorts, no dose-limiting toxic effects occurred at the doses evaluated. An additional 89 patients were treated in five expansion cohorts. Among 99 patients with T790M mutation, objective response rate (ORR) was 66% [95% confidence interval (CI), 56.9–75.2] across all dose levels (20–320 mg once daily). In particular, ORR was 71% at a dose of 240 mg once daily whereas deep responses were seen in low doses (40–120 mg). In patients with BM, the intracranial ORR was 50% across all dose levels (95% CI, 21.1–78.9). Consistent with our mouse safety data, YH25448 demonstrated a good safety profile and tolerability without dose-limiting toxicity observed up to 320 mg. Although it always needs a great caution when comparing results between different clinical trials, the frequency of overall treatment-related adverse events (AE) and treatment-related grade 3 to 5 AEs were numerically lower than osimertinib phase I/II trial (69% vs. 80% and 3% vs. 13%; refs. 9, 26). In addition, the incidences of skin rash and diarrhea which are commonly observed in EGFR-TKIs were lower in YH25448 compared with osimertinib, respectively (26% vs. 40% for any grade skin rash and 13% vs. 47% in any grade diarrhea). Most AEs of patients treated with YH25448 were grade 1 or 2 (9, 26). YH25448, as a mono-anilino–pyrimidine compound structurally similar to osimertinib, irreversibly binds to the EGFR kinase by targeting the cysteine-797 residue in the ATP binding site via covalent bond formation (Fig. 1A). The substitution of cysteine with serine at codon 797 (C797S) is a common resistance mechanism to osimertinib, because C797S mutation prevents formation of a covalent bond between osimertinib and the thiol group (–SH) of cysteine in the *EGFR* C797 residue (38). Therefore, considering the similar binding mode, C797S mutation is anticipated to confer resistance to YH25448. As expected, osimertinib-resistant, C797S-mutant YU-1097 cells was cross-resistant to YH25448 (Fig. 2B).

In conclusion, we demonstrated that YH25448 is a novel, highly potent, BBB-penetrating, irreversible EGFR-TKI, which selectively blocks *EGFR* sensitizing and T790M mutations. The comparable potency and CNS activity, with the possibility of a wider therapeutic index, of YH25448 to osimertinib strongly support further clinical development of YH25448 for the treatment of EGFR-mutant NSCLC.

Disclosure of Potential Conflicts of Interest

S. Oh is an employee of Yuhan Corporation. No potential conflicts of interest were disclosed by the other authors.

Authors' Contributions

Conception and design: J. Yun, J.S. Koh, H.-J. Song, Y.-S. Lee, S.-W. Oh, S. Choi, H.R. Kim, B.C. Cho
Development of methodology: K.-H. Pyo, B.C. Cho
Acquisition of data (provided animals, acquired and managed patients, provided facilities, etc.): M.H. Hong, H.N. Kang, S.S. Lee, Y.-S. Lee, B.C. Cho
Analysis and interpretation of data (e.g., statistical analysis, biostatistics, computational analysis): J. Yun, S.-Y. Kim, C.-W. Park, S. Kim, S. Choi, B.C. Cho
Writing, review, and/or revision of the manuscript: J. Yun, M.H. Hong, D.K. Kim, Y.-S. Lee, S.-W. Oh, H.R. Kim, B.C. Cho
Administrative, technical, or material support (i.e., reporting or organizing data, constructing databases): M.H. Hong, D.K. Kim, B.C. Cho
Study supervision: H.-J. Song, S.-W. Oh, S. Choi, H.R. Kim, B.C. Cho
Other (generation of patient-derived cell models): S.-Y. Kim

Acknowledgments

This research was supported by Basic Science Research Program through the National Research Foundation of Korea (NRF) funded by the Ministry of Science, ICT & Future Planning (2016R1A2B3016282), Republic of Korea, and by Korea Drug Development Fund (KDDF) funded by MSIT, MOTIE, and MOHW (Grant No. 201803-05), Republic of Korea.

The costs of publication of this article were defrayed in part by the payment of page charges. This article must therefore be hereby marked *advertisement* in accordance with 18 U.S.C. Section 1734 solely to indicate this fact.

Received September 10, 2018; revised October 31, 2018; accepted January 16, 2019; published first January 22, 2019.

References

1. Novello S, Barlesi F, Califano R, Cufer T, Ekman S, Levra MG, et al. Metastatic non-small-cell lung cancer: ESMO Clinical Practice Guidelines for diagnosis, treatment and follow-up. Ann Oncol 2016;27:v1–v27.
2. Mok TS, Wu YL, Thongprasert S, Yang CH, Chu DT, Saijo N, et al. Gefitinib or carboplatin-paclitaxel in pulmonary adenocarcinoma. N Engl J Med 2009;361:947–57.
3. Rosell R, Carcereny E, Gervais R, Vergnenegre A, Massuti B, Felip E, et al. Erlotinib versus standard chemotherapy as first-line treatment for European patients with advanced EGFR mutation-positive non-small-cell lung cancer (EURTAC): a multicentre, open-label, randomised phase 3 trial. Lancet Oncol 2012;13:239–46.
4. Yang JC, Wu YL, Schuler M, Sebastian M, Popat S, Yamamoto N, et al. Afatinib versus cisplatin-based chemotherapy for EGFR mutation-positive lung adenocarcinoma (LUX-Lung 3 and LUX-Lung 6): analysis of overall survival data from two randomised, phase 3 trials. Lancet Oncol 2015;16:141–51.
5. Wu YL, Cheng Y, Zhou X, Lee KH, Nakagawa K, Niho S, et al. Dacomitinib versus gefitinib as first-line treatment for patients with EGFR-mutation-positive non-small-cell lung cancer (ARCHER 1050): a randomised, open-label, phase 3 trial. Lancet Oncol 2017;18:1454–66.
6. Lim SM, Syn NL, Cho BC, Soo RA. Acquired resistance to EGFR targeted therapy in non-small cell lung cancer: mechanisms and therapeutic strategies. Cancer Treat Rev 2018;65:1–10.
7. Westover D, Zugazagoitia J, Cho BC, Lovly CM, Paz-Ares L. Mechanisms of acquired resistance to first- and second-generation EGFR tyrosine kinase inhibitors. Ann Oncol 2018;29:i10–i9.
8. Kim ES. Olmutinib: first global approval. Drugs 2016;76:1153–7.
9. Janne PA, Yang JC, Kim DW, Planchard D, Ohe Y, Ramalingam SS, et al. AZD9291 in EGFR inhibitor-resistant non-small-cell lung cancer. N Engl J Med 2015;372:1689–99.
10. Sequist LV, Soria JC, Goldman JW, Wakelee HA, Gadgeel SM, Varga A, et al. Rociletinib in EGFR-mutated non-small-cell lung cancer. N Engl J Med 2015;372:1700–9.
11. O'Kane GM, Barnes TA, Leighl NB. Resistance to epidermal growth factor receptor tyrosine kinase inhibitors, T790M, and clinical trials. Curr Oncol 2018;25:S28–S37.
12. Mok TS, Wu YL, Ahn MJ, Garassino MC, Kim HR, Ramalingam SS, et al. Osimertinib or platinum-pemetrexed in EGFR T790M-positive lung cancer. N Engl J Med 2017;376:629–40.
13. Soria JC, Ohe Y, Vansteenkiste J, Reungwetwattana T, Chewaskulyong B, Lee KH, et al. Osimertinib in untreated EGFR-mutated advanced non-small-cell lung cancer. N Engl J Med 2018;378:113–25.
14. Ferrara R, Mezquita L, Besse B. Progress in the management of advanced thoracic malignancies in 2017. J Thorac Oncol 2018;13:301–22.
15. Kotake M, Murakami H, Kenmotsu H, Naito T, Takahashi T. High incidence of interstitial lung disease following practical use of osimertinib in patients who had undergone immediate prior nivolumab therapy. Ann Oncol 2017;28:669–70.
16. Heon S, Yeap BY, Britt GJ, Costa DB, Rabin MS, Jackman DM, et al. Development of central nervous system metastases in patients with advanced non-small cell lung cancer and somatic EGFR mutations treated with gefitinib or erlotinib. Clin Cancer Res 2010;16:5873–82.
17. Lee YJ, Choi HJ, Kim SK, Chang J, Moon JW, Park IK, et al. Frequent central nervous system failure after clinical benefit with epidermal growth factor receptor tyrosine kinase inhibitors in Korean patients with nonsmall-cell lung cancer. Cancer 2010;116:1336–43.
18. Di L, Rong H, Feng B. Demystifying brain penetration in central nervous system drug discovery. Miniperspective. J Med Chem 2013;56:2–12.
19. Togashi Y, Masago K, Fukudo M, Terada T, Fujita S, Irisa K, et al. Cerebrospinal fluid concentration of erlotinib and its active metabolite OSI-420 in patients with central nervous system metastases of non-small cell lung cancer. J Thorac Oncol 2010;5:950–5.
20. Ballard P, Yates JW, Yang Z, Kim DW, Yang JC, Cantarini M, et al. Preclinical comparison of osimertinib with other EGFR-TKIs in EGFR-mutant NSCLC brain metastases models, and early evidence of clinical brain metastases activity. Clin Cancer Res 2016;22:5130–40.
21. Tan CS, Cho BC, Soo RA. Treatment options for EGFR mutant NSCLC with CNS involvement-Can patients BLOOM with the use of next generation EGFR TKIs? Lung Cancer 2017;108:29–37.
22. Uchibori K, Inase N, Araki M, Kamada M, Sato S, Okuno Y, et al. Brigatinib combined with anti-EGFR antibody overcomes osimertinib resistance in EGFR-mutated non-small-cell lung cancer. Nat Commun 2017;8:14768.
23. Hirano T, Yasuda H, Tani T, Hamamoto J, Oashi A, Ishioka K, et al. In vitro modeling to determine mutation specificity of EGFR tyrosine kinase inhibitors against clinically relevant EGFR mutants in non-small-cell lung cancer. Oncotarget 2015;6:38789–803.
24. Saxon JA, Sholl LM, Janne PA. EGFR L858M/L861Q cis mutations confer selective sensitivity to afatinib. J Thorac Oncol 2017;12:884–9.
25. Ercan D, Xu C, Yanagita M, Monast CS, Pratilas CA, Montero J, et al. Reactivation of ERK signaling causes resistance to EGFR kinase inhibitors. Cancer Discov 2012;2:934–47.
26. Cho BC, Han JY, Kim SW, Lee KH, Kim DW, Lee YG, et al. Lazertinib, a third generation EGFR-TKI, in patients with EGFR-TKI-resistant NSCLC: updated results of a phase I/II study. Presented at IASLC 19th World Conference on Lung Cancer, Abstract #12817. September 23–26, 2018, Toronto, Canada.
27. Nanney LB, Stoscheck CM, King LE, Underwood RA, Holbrook KA. Immunolocalization of epidermal growth-factor receptors in normal developing human skin. J Invest Dermatol 1990;94:742–8.
28. Sullivan I, Planchard D. Osimertinib in the treatment of patients with epidermal growth factor receptor T790M mutation-positive metastatic non-small cell lung cancer: clinical trial evidence and experience. Ther Adv Respir Dis 2016;10:549–65.
29. Holcmann M, Sibilia M. Mechanisms underlying skin disorders induced by EGFR inhibitors. Mol Cell Oncol 2015;2:e1004969.
30. Kozuki T. Skin problems and EGFR-tyrosine kinase inhibitor. Jpn J Clin Oncol 2016;46:291–8.
31. Melosky B, Leighl NB, Rothenstein J, Sangha R, Stewart D, Papp K. Management of EGFR-TKI-induced dermatologic adverse events. Curr Oncol 2015;22:123–32.
32. Pastore S, Mascia F, Mariani V, Girolomoni G. The epidermal growth factor receptor system in skin repair and inflammation. J Invest Dermatol 2008;128:1365–74.

33. Ramalingam SS, Yang JCH, Lee CK, Kurata T, Kim DW, John T, et al. Osimertinib as first-line treatment of EGFR mutation-positive advanced non-small-cell lung cancer. J Clin Oncol 2018;36:841–9.
34. Cho BC, Chewaskulyong B, Lee KH, Dechaphunkul A, Sriuranpong V, Imamura F, et al. Osimertinib vs standard of care (SoC) EGFR-TKI as first-line treatment in patients with EGFR-TKI sensitising mutation (EGFRm) positive advanced non-small cell lung cancer (NSCLC): FLAURA Asian subset. Ann Oncol 2017;28:(Suppl 10):186–195.
35. Sequist LV, Yang JC, Yamamoto N, O'Byrne K, Hirsh V, Mok T, et al. Phase III study of afatinib or cisplatin plus pemetrexed in patients with metastatic lung adenocarcinoma with EGFR mutations. J Clin Oncol 2013;31:3327–34.
36. Wu YL, Zhou C, Hu CP, Feng J, Lu S, Huang Y, et al. Afatinib versus cisplatin plus gemcitabine for first-line treatment of Asian patients with advanced non-small-cell lung cancer harbouring EGFR mutations (LUX-Lung 6): an open-label, randomised phase 3 trial. Lancet Oncol 2014; 15:213–22.
37. Lacouture ME. Mechanisms of cutaneous toxicities to EGFR inhibitors. Nat Rev Cancer 2006;6:803–12.
38. Thress KS, Paweletz CP, Felip E, Cho BC, Stetson D, Dougherty B, et al. Acquired EGFR C797S mutation mediates resistance to AZD9291 in non-small cell lung cancer harboring EGFR T790M. Nat Med 2015;21: 560–2.

Published OnlineFirst January 22, 2019; DOI: 10.1158/1078-0432.CCR-18-2906

Clinical Cancer Research

YH25448, an Irreversible EGFR-TKI with Potent Intracranial Activity in EGFR Mutant Non–Small Cell Lung Cancer

Jiyeon Yun, Min Hee Hong, Seok-Young Kim, et al.

Clin Cancer Res 2019;25:2575-2587. Published OnlineFirst January 22, 2019.